IOPscience iopscience.iop.org

Home Search Collections Journals About Contact us My IOPscience

Undetectability of the P_{b1} point defect as an interface state in thermal $(100)Si/SiO_2$

This article has been downloaded from IOPscience. Please scroll down to see the full text article.

1998 J. Phys.: Condens. Matter 10 L19

(http://iopscience.iop.org/0953-8984/10/1/003)

View the table of contents for this issue, or go to the journal homepage for more

Download details:
IP Address: 171.66.16.209
The article was downloaded on 14/05/2010 at 11:52

Please note that terms and conditions apply.

LETTER TO THE EDITOR

Undetectability of the P_{b1} point defect as an interface state in thermal (100)Si/SiO_2

A Stesmans and V V Afanas'ev
Department of Physics, University of Leuven, 3001 Leuven, Belgium

Received 19 August 1997, in final form 20 October 1997

Abstract. The electrical activity of the electron-spin-resonance-active interfacial point defects P_{b0} and P_{b1} (unpaired Si bonds) has been examined on standard thermal (100)Si/SiO_2. After elimination of the H-passivation factor, this has been achieved through combination of electrical and ESR analysis on common suites of samples exhibiting a distinct controlled variation, both relatively and absolutely, of the P_{b0} and P_{b1} densities. Unlike initial inference, it is found that P_{b1} is electrically inactive as a degrading interface state; hence it has no direct electrical influence in Si/SiO_2-based device physics. All P_{b0} defects, however, are found to be electrically active, putting these EPR-active defects in a unique position.

With progressing metal-oxide–semiconductor (MOS) technology, the crucial role of the phenomena occurring at the interface of the basic Si/SiO_2 entity has become ever more important, an issue more pertinent than ever in view of the incessant trend for down-scaling [1]. Of specific concern are the electrically active interface defects, with electronic states in the Si band gap, as they may operate as trapping and recombination centres, thus adversely affecting critical current [2]. They are seen as naturally introduced during oxidation as a result of lattice–network mismatch [3].

Over the many years, these, of course, have been most intensely studied with repect to their electric impact, which has resulted in a thorough characterization incorporating trap density, distribution and energy levels [1, 2]. However, for those states associated with magnetically active sites, the information as to their *atomic identity* has almost exclusively come from electron spin resonance (ESR) investigation [2–10].

At the (111)Si/SiO_2 interface, only one point defect has so far been isolated by ESR [2, 4, 6], termed P_b and conclusively identified as a threefold coordinated interfacial Si ($\cdot$Si $\equiv Si_3$). Analysis by the capacitance–voltage (CV) technique in conjunction with ESR has ascertained it as an amphoteric trap of effective electron–electron correlation energy $U_e = 0.5$ eV, with the $+/0$ and $0/-$ levels in the Si bandgap at 0.3 and 0.8 eV above the valence band level E_v, respectively. The P_b defects are established to be the source of about 50% of the interface traps [11, 12]

In the technologically dominant (100)Si/SiO_2 ESR has delineated two different species, termed P_{b0} and P_{b1} [5]. Initial analogous research [13] as conducted on P_b had also concluded both types to imply detrimental interface states with the significant $+/0$ and $0/-$ levels at $E_v + 0.3$ and $E_v + 0.85$ eV, and $E_v + 0.45$ and $E_v + 0.8$ eV, complying with $U_e = 0.55$ and 0.35 eV for P_{b0} and P_{b1}, respectively; repeated combination of electrical and ESR work has left little doubt about this assignment for P_{b0}. Also here, initial research had promoted these defects, physically located at the very interface, as responsible for the

majority of all interface states [12, 13]. However, as already hinted initially [11,13], it has now become clear that, with inclusion of all traps residing in more remote interfacial SiO_2 layers, P_{b0} and P_{b1} do not set the full scene; neither do the P_b defects in (111)Si/SiO_2; other interface states [14] emerge, of which most have apparently so far escaped ESR detection. Within this increasingly complicating picture, particularly the role of P_{b1} has become hazy, to say the least, as exposed by various experimental observations over many years [15–19]. The initial (to our knowledge thus far the sole) conclusion about P_{b1}'s electrical activity has been inferred from electrical (CV) research in conjunction with ESR on selected samples in combination with appropriate anodic or corona biasing. It may then appear somewhat surprising that, in the light of the paramount importance for the understanding of (100)Si/SiO_2-based device physics, this conclusion has since not been revisited for corroboration. The likely reason lies in the involved complexity (e.g., signal-to-noise ratio, overlapping signals) of the ESR spectroscopy in combination with the previous general failure to establish unquestionable relationships between processing parameters and incorporated P_{b0} and P_{b1} densitities [2, 5, 12].

It is clear, though, that any attempt for further insight would much benefit from understanding of the electrical role of the thus-far-isolated ESR-active defects, i.e., P_{b1}. This is the focus of the present work. In a most straightforward way, we have carried out electrical (CV) and ESR analysis on the same sample sets of standard thermal (100)Si/SiO_2 as a function of controlled, monotonic variation in the density, both relatively and absolutely, of the physically present P_{b0} and P_{b1} ensembles. It appears an approach with fewest complications; there are no threats such as possibly arising from less defined biasing procedures or oxidation-induced sample-to-sample variations. This has been possible as a result of a recent clear isolation of a processing parameter, enabling the relative density of the P_{b0} and P_{b1} systems to be controlled through simple postoxidation annealing. As a major result, it is found the P_{b1} defect plays no significant role in the interface state activity.

Samples studied were commercial 2 inch diameter two-side-polished float-zone (100)Si wafers (>100 Ωcm; p type). For ESR purposes, these were sliced in 2×9 mm^2 pieces. After appropriate cleaning, including a 10 min treatment in Piranha etch at 80 °C, the samples were thermally oxidized at ≃970 °C (99.999% O_2; 1.1 atm) to an oxide thickness $d_{ox} \sim 50$ nm. Both (100)Si/SiO_2 structures grown in a local high-vacuum laboratory and a technological facility [20] were studied, with identical results. For the reliable determination of the total interface trap density N_{it} (*vide infra*), both p- and n-type samples (0.05–120 Ωcm) were coprocessed. After a first ESR diagnosis in the as-oxidized state, the samples were subjected to various annealing steps in vacuum ($\lesssim 4\times10^{-7}$ Torr) for ≃1 h each at desired temperatures in the range 620–1110 °C to establish sets of samples with the intrinsic densities P_{b0} and P_{b1} varying in a controlled, systematic manner; such a trend is illustrated in figure 1 by typical 4.3 K ESR spectra , labelled by the temperature T_a of the final vacuum anneal. Since vacuum annealing in the 620–1110 °C range was the last applied thermal step, this assured exhaustive ESR activation of the P_{b0} and P_{b1} ensembles (dissociation of H-passivated entities) [7], thus eliminating any possibly adverse influence of the H-passivation factor. Each ESR sample was started from freshly oxidized slices. More details can be found elsewhere [3, 9].

Conventional absorption mode ESR (≃20.1 GHz) observations were made at 4.3 K, as described elsewhere [3, 9]. Spectroscopically correct spectra, devoid of noticeable saturation or overmodulation effects, were recorded by reducing the incident microwave power ($P < 0.15$ nW) and magnetic field modulation amplitude (<0.25 G; ≃100 kHz) to linear response levels. The results were obtained with the applied magnetic field $\boldsymbol{B} \perp$ (100)Si/SiO_2 interface (within 3°), the simplest spectrum case; for each of the two defect types, P_{b0} and P_{b1}, the various g branches (equivalent defect orientations) then

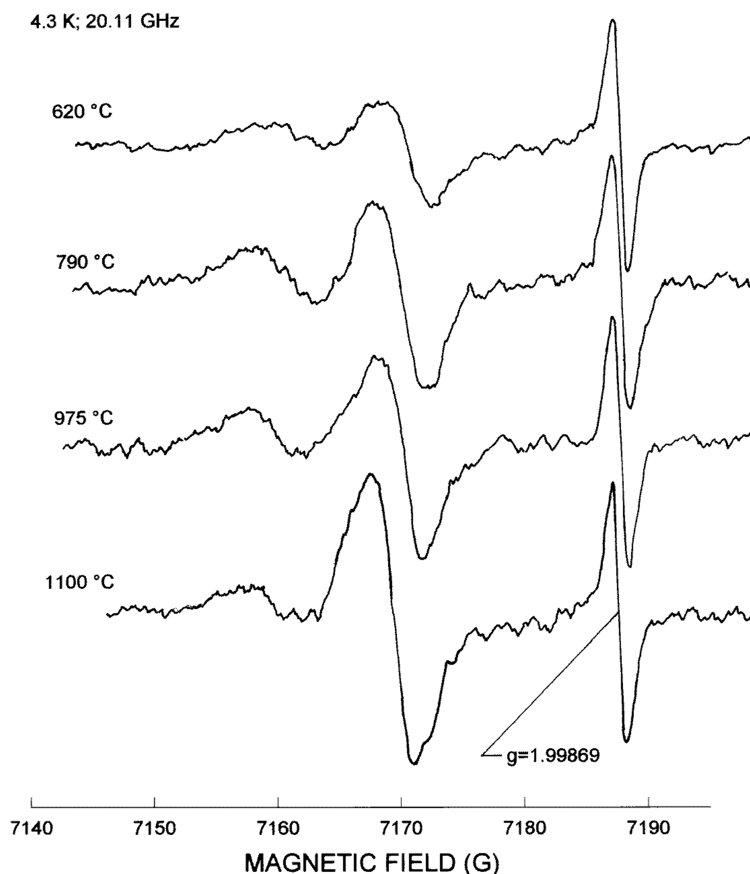

Figure 1. Typical absorption-derivative ESR spectra ($P_\mu < 0.15$ nW), measured with $\boldsymbol{B}$ normal to the interface, of a set of standard thermal (100)Si/SiO_2 samples (1.1 atm O_2; dry; $\sim 970\,^\circ$C), illustrating the controlled variation in the density of of P_{b0} and P_{b1} entities. The spectra are measured under identical spectroscopical conditions and labelled with the temperature of the final post-oxidation anneal in vacuum. The signal at $g = 1.998\,69$ stems from a fixed intensity marker.

coincide, resulting in a two-line spectrum, thus providing optimum sensitivity and spectral resolution. Areal defect (spin) densities were determined by double numerical integration of the recorded first-absorption-derivative responses relative to the signal of a fixed comounted isotropic Si:P standard ($g(4.2\text{ K}) = 1.998\,69 \pm 0.000\,02$) recorded in one trace. Combination with an appropriate integration algorithm resulted in reliable data for P_{b0} and P_{b1} separately. Absolute and relative accuracy of spin density determination is estimated at $\simeq$10% and 5%, respectively.

N_{it} was determined from 1 MHz CV measurements at 300 and 77 K on Si/SiO_2/Au structures (evaporated circular Au electrodes of diameter $\simeq$ 0.8 mm). The temperature lowering causes a shift of the Fermi level E_F in Si towards the edge of the bandgap, and accordingly, a shift in the flatband point on the CV curve. However, if there are interface states within this energy interval of E_F variation they will recharge and cause an additional CV curve shift from which N_{it} can be determined (Gray–Brown technique) [21]. For the

doping concentrations of the studied n- and p-type Si crystals (ranging from 1×10^{14} to 2×10^{17} cm^{-3}), this method allows N_{it} determination in two energy windows ranging from 0.02 to 0.35 eV from both edges of the Si bandgap [22]. This approach proves most direct and reliable to determine N_{it}, as no suppositions are involved; the integration of the interface state density over the scanned energy range is performed *physically* rather than numerically; no detailed spectral information is sought. Three other advantages of the Gray–Brown technique may be worthy of notice: (i) it allows detection of the interface states close (>20 meV) to the Si bandgap edges, i.e., an energy range inaccessible for room-temperature CV techniques; (ii) the method does not suffer from the significant uncertainty in the Si surface potential determination near the band edges in the case of high N_{it}, inherent to low-frequency CV measurements; (iii) the high-frequency condition, necessary for correct determination of the flatband voltage value, is more easily met at 77 K than at room temperature. Therefore, the Gray–Brown approach is considered the most appropriate way to determine the *total* density of electrically active Si/SiO_2 interface states. For clarity, we add that N_{it} was not only determined upon vacuum annealing, but also after passivation of the P_b-type centres by hydrogen. The latter leads to $N_{it} < 3 \times 10^{10}$ and 5×10^{10} cm^{-2} for (100) and (111)Si/SiO_2, respectively, thus setting an upper limit to the density of interface states related to defects other than P_b-type defects.

To further ensure correct N_{it} determination, we compared the values obtained from the Gray–Brown technique with the total interface state density in the Si bandgap derived from the difference in flatband voltages on 77 K CV curves of both n- and p-type samples. This difference corresponds to the shift of the Fermi level across 95% of the Si bandgap and recharging of *all* interface states within this range. Typically, the total interface state density and that obtained from the Gray–Brown method (N_{it}(n type) + N_{it}(p type)) is found to differ by less than 20%. Therefore, we will only present the numbers determined by the Gray–Brown method.

The key results are shown in figure 2, where in panel (a) is depicted the behaviour of the P_{b0} and P_{b1} densities as a function of T_a. Remarkably, [P_{b1}] is seen to exhibit a pronounced increase (about 4.5-fold) with T_a, growing from $\simeq 1.3 \times 10^{12}$ cm^{-2}—about the as-grown value—to about 6×10^{12} cm^{-2} at 1110 °C. The P_{b0} density, by contrast, hardly varies, starting at [P_{b0}] $\simeq 9 \times 10^{11}$ cm^{-2} at about 620 °C, showing, if anything, a slight tendency to decrease with raising T_a. Overall, the total P_{b0} and P_{b1} density increases from $\simeq$2.3 to 6.7×10^{12} cm^{-2}—roughly a threefold increase. Figure 2(b) presents the results on N_{it} for both p- and n-type samples: the top panel corresponds to the ESR samples studied in figure 2(a). An important remark here is that the oxide charge was found to be negligible ($< 1 \times 10^{11}$ cm^{-2}) in all samples, thus excluding a possible adverse effect on the occupancy of the interface levels, and associated magnetic states, as a result of band-bending-induced level shift. When comparing both panels, a general remark is that the n-Si and p-Si data appear as perfect mirror images, adding confidence in the inferred N_{it} data; moreover, it affirms the electrically active interface defects to be amphoteric with a level both in the upper and lower half of the bandgap.

When comparing figures 2(a) and (b), the results are as clear as they are remarkable. First, no variation is discerned in N_{it}(100) within error bars, which, when confronted with the ESR data, excludes contribution of P_{b1} to N_{it}—substantial evidence that P_{b1} is insignificant as an electrical interface state. The particular densities involved (i.e., the large P_{b1} density in the high-temperature anneal range) exclude a counterbalancing interference during annealing by interface states of different nature. Second, and in sharp contrast, is the notably close tracking—both in trend and numbers—of [P_{b0}] by N_{it}, convincing evidence, as expected [12,13], that *all* P_{b0} defects are electrically operative as interface states.

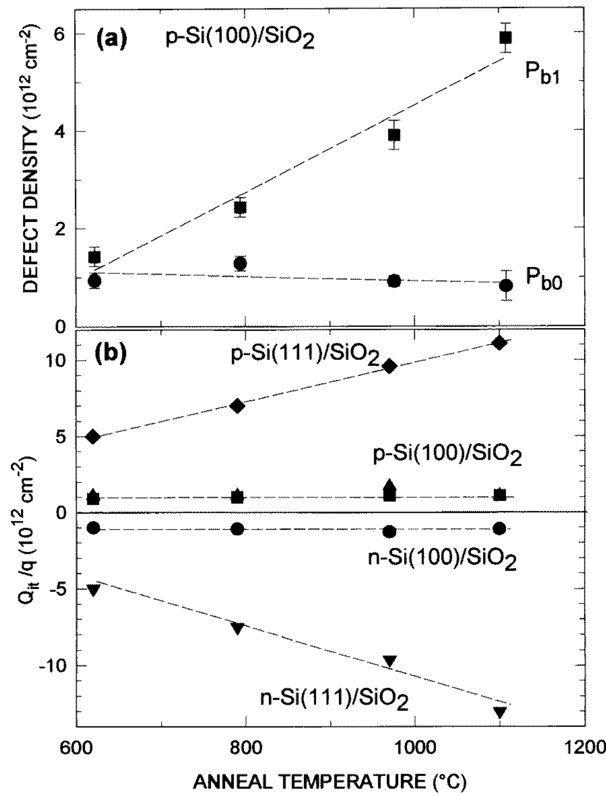

Figure 2. (a) Plot of ESR intensities of P_{b0} and P_{b1} interface defects in thermal p-type (100)Si/SiO_2 versus the final vacuum annealing temperature; (b) areal interface state density measured electrically (low-temperature CV) on various sets of coprocessed p- and n-type (100) and (111)Si/SiO_2 structures. The samples of the top panel are those of figure 1. The lines are guides to the eye.

For the sake of comparison, we have also included in figure 2(b) N_{it} values on n- and p-type (111)Si/SiO_2, of which the ESR data have been presented elsewhere [23]. The increase in P_b ($\cdot$Si $\equiv$$Si_3$) density with increasing T_a is perfectly reproduced by N_{it} in both halves of the Si bandgap, reaffirming P_b defects as amphoteric interface states in (111)Si/SiO_2.

It needs to be added though that the fact that all P_{b0} defects appear electrically active does not imply the P_{b0} defect to be the sole interface state of significance; all P_{b0} defects appear as electrical interface states, but not vice versa. Clearly, when H passivation of the P_{b0} ensemble is applied, reducing their unpassivated part to the sub-10^{10} cm^{-2} range, other (perhaps less numerous) interface traps may be revealed, or even become dominant. Or, as hinted from the reactive impact of H on the Si/SiO_2 entity, new defects, now likely in near-interfacial SiO_2 layers, may simply be generated in increasing numbers [14, 18, 24].

Clearly, a major inference from our work is the electrical inactivity of the P_{b1} defect in regard to any role as a source of N_{it}. This is at odds with the conclusion in early (and so far, sole) work [11, 13]. In that work, the relation between P_b and P_{b0} versus N_{it} was analysed with gated MOS capacitors: large ESR capacitors and small N_{it} capacitors on the same chip, from where convincing correlation between P_b, P_{b0} and N_{it} was provided. These conclusions, confirmed here, have not since been contested elsewhere. However,

because of weak ESR signals, an indirect method involving corona charging was used for P_{b1}, and it required several dissimilar samples. Not only is this a harsh method, possibly inducing passivation and depassivation of P_b-like centres via H-based reactions [8, 25], but the much less controllable method would cause considerable loss of precision, and prevent any immediate indication of whether or not a P_{b1} contribution to N_{it} was, in fact, implied by the overall correlations.

A further factor in the early work was the unconsidered possibility that P_{b1} was located farther from the interface, and that it would not respond in the relatively fast CV measurements, even though the electron occupancy at the centre would respond to the gate bias on the slow time scale of ESR [12]. It would have been no surprise at that time if P_{b1} were *not* a source of N_{it}. Indeed, there was still some disbelief that any P_b-like centres were contributors. At the present time, of course, with the role of P_b widely accepted, our discovery comes as a surprise.

Another potential inaccuracy could have come from having used the ESR signal amplitude, rather than signal integration (area under absorption curve), as intensity (defect density) measure; this has been shown to be incorrect [8] as a result of line shape variations due to the altering impact of dipole–dipole interaction with varying spin densities. However, for the typical low P_b-type defect densities studied in (100)Si/SiO_2, that effect should be negligible.

The finding of the electrical inactivity of P_{b1} as an interface state may alleviate a number of obscurities regarding this matter accumulated experimentally (mainly electrically) over many years since the initial assignment. We just list a few by way of illustration.

(1) Recent high-resolution wide-frequency-range (1–10^7 Hz) conductance measurements on MOS capacitors formed on fully depassivated (700 °C; 2 h) thermal (100)Si/SiO_2 structures failed to resolve two defect types; so, should P_{b0} and P_{b1} be equally active as electrical interface states, they then must exhibit indistinguishable capture cross sections [15].

(2) Next, there are the results of electrically detected magnetic resonance (EDMR), based on the spin dependent recombination (SDR) phenomenon, an excellent technique for direct detection of the electrical activity of the interface defects as a magnetic resonance signal in the electrical current. At the (100)Si/SiO_2 interface, only one signal ascribed to P_{b0} could be observed; the technique has so far failed to resolve a P_{b1} signal, despite intense efforts [16, 17, 19]. As a way out, one could invoke speculative arguments such as unequal effectivity of interface damaging (e.g., electron irradiation, hot-electron stress, ion implantation) in P_{b0} and P_{b1} production, excessive line width of unknown origin broadening the signal beyond detection or vaguely described drastic differences in characteristic response times affecting the SDR process for both types of defect differently so as to erode the P_{b1} signal. The present result, however, explains at once why P_{b1} remains EDMR undetectable.

(3) The results might also redirect theory. The theoretical modelling of P_{b1} has been addressed in an impressive work [26] calculating five cluster models for the defect using molecular orbital techniques. Here, a main experimental guide was the presumed electrical level in the bandgap. For example on this basis the initial Poindexter model $\cdot$Si $\equiv Si_2O$ and the strain relief model SB_2 were not retained, while the strained bond (SB_1) model was further considered. This might need revision, as the P_{b1} defect now appears not to be an amphoteric trap with electrical levels deep in the gap, separated by a substantial positive U_e.

In summary, from a least-complicated experimental approach, substantial evidence has been provided that, unlike earlier belief, the ESR-active P_{b1} defect is not a detrimental

amphoteric electrically active interface defect. In addition, the work has provided a clue to tuning the P_b-type defect desity in a controlled systematic way, stimulating experimental progress. While the former inference will likely remove it somewhat from the intensely visited array of interface defects of interest to device physics, the striving for its atomic identification does not necessarily become less important. Indeed, if not of electrical significance, it still concerns an interfacial point defect intrinsically introduced in large numbers to account for interface mismatch. Understanding its atomic structure may add to unveiling the still poorly comprehended physical structure of the (100)Si/SiO_2 interface. Evaluating the role of P_{b1} in this scheme may help unveiling the basic reason as to why (100)Si/SiO_2 is the overruling interface of choice for device fabrication.

References

[1] For a review on Si/SiO_2 defect physics, see the 13 papers in *Semicond. Sci. Technol.* **4** (1989) 961, and references therein.
[2] Poindexter E and Caplan P 1983 *Prog. Surf. Sci.* **14** 211
Helms R and Poindexter E 1994 *Rep. Prog. Phys.* **57** 791
[3] Stesmans A 1993 *Phys. Rev.* B **48** 2418
Stesmans A 1993 *Phys. Rev. Lett.* **70** 1723
[4] Caplan P, Poindexter E, Deal B and Razouk R 1979 *J. Appl. Phys.* **50** 5847
[5] Poindexter E, Caplan P, Deal B and Razouk R 1981 *J. Appl. Phys.* **52** 879
[6] Brower K 1983 *Appl. Phys. Lett.* **43** 1111
[7] Brower K L 1988 *Phys. Rev.* B **38** 9657
Brower K L 1990 *Phys. Rev.* B **42** 3444
[8] Stesmans A 1996 *Appl. Phys. Lett.* **68** 2723
Stesmans A 1996 *Appl. Phys. Lett.* **68** 2076
[9] Van Gorp G and Stesmans A 1992 *Phys. Rev.* B **45** 4344
[10] Carlos W E 1987 *Appl. Phys. Lett.* **50** 1450
[11] Poindexter E H, Gerardi G J, Rueckel M-E, Caplan P J, Johnson N M and Biegelsen D K 1984 *J. Appl. Phys.* **56** 2844
[12] Poindexter E H 1989 *Semicond. Sci. Technol.* **4** 961
[13] Gerardi G J, Poindexter E H, Caplan P J and Johnson N M 1986 *Appl. Phys. Lett.* **49** 348
[14] Sah C-T, Sun J Y-C and Tsou J J-T 1984 *J. Appl. Phys.* **55** 1525
Trombetta L, Gerardi G, DiMaria D J and Tierney E 1988 *J. Appl. Phys.* **64** 2434
[15] Uren M J, Brunson K M, Stathis J H and Cartier E 1997 *Microelectron. Eng.* **36** 219
[16] Vranch R L, Henderson B and Pepper M 1988 *Appl. Phys. Lett.* **52** 1161
Vuillaume D, Deresmes D and Stiévenard D 1994 *Appl. Phys. Lett.* **64** 1690
[17] Krick J T, Lenahan P M and Dunn G J 1991 *Appl. Phys. Lett.* **59** 3437
[18] Stathis J H and Cartier E 1994 *Phys. Rev. Lett.* **72** 2745
[19] Stathis J H and DiMaria D J 1992 *Appl. Phys. Lett.* **61** 2887
[20] DIMES, Delft, The Netherlands
[21] Gray P V and Brown D M 1966 *Appl. Phys. Lett.* **8** 31
[22] Landsberg P T 1991 *Recombination in Semiconductors* (Cambridge: Cambridge University Press)
[23] Stesmans A and Afanas'ev V V 1996 *Phys. Rev.* B **54** R11 129
[24] Griscom D L 1992 *J. Electron. Matter* **21** 762
Nissan-Cohen Y and Gorczyca T 1988 *IEEE Electron Device Lett.* **9** 287
[25] Williams R 1974 *J. Vac. Sci. Technol.* **11** 1025
[26] Edwards A H 1988 *The Physics and Chemistry of* SiO_2 *and the* SiO_2 *Interface* ed C R Helms and B E Deal (New York: Plenum) p 271